

D. J. Wever
A. G. Veldhuizen
J. P. Klein
P. J. Webb
G. Nijenbanning
J. C. Cool
J. R. v. Horn

A biomechanical analysis of the vertebral and rib deformities in structural scoliosis

Received: 19 October 1998
Revised: 29 January 1999
Accepted: 10 February 1999

D. J. Wever · A. G. Veldhuizen (✉)
J. R. v. Horn
Department of Orthopaedics,
University Hospital Groningen,
P.O. Box 30.001,
NL-9700 RB Groningen, The Netherlands
Tel.: +31 50-3612802,
Fax: +31 50-3611737

J. P. Klein
Department of Radiology,
University Hospital of Groningen,
The Netherlands

P. J. Webb
Backpain Service,
Taunton and Somerset NHS Trust,
Taunton,
UK

G. Nijenbanning · J. C. Cool
Institute for Biomedical Technology,
University of Twente,
The Netherlands

Abstract Although the structural changes occurring in the scoliotic spine have been reported as early as the 19th century, the descriptions and biomechanical explanations have not always been complete and consistent. In this study, three-dimensionally rendered CT images of two human skeletons with a scoliotic deformity and two patients with serious scoliosis were used to describe the intrinsic vertebral and rib deformities. The pattern of structural deformities was found to be consistent. Apart from the wedge deformation of the apical vertebrae, a rotation deformity was found in the transversal plane between the vertebral body and the posterior complex: the vertebral body was maximally rotated towards the convexity of the scoliotic curve, whereas the tip of the spinous process was pointed to posterior. The rib deformities at the convex side of

the scoliotic curve showed an increased angulation of the rib at the posterior angle, whereas the rib curve on the concave side was flattened. The observed vertebral deformities suggest that these are caused by bone remodelling processes due to forces in the anterior spinal column, which drive the apical vertebral body out of the midline, whereas forces of the musculo-ligamentous structures at the posterior side of the spinal column attempt to minimize the deviations and rotations of the vertebrae. The demonstrated rib deformities suggest an adaptation to forces imposed by the scoliotic spine.

Key words Scoliosis · Scoliosis, deformity · Scoliosis, vertebra · Scoliosis, rib · Scoliosis, biomechanics

Introduction

Idiopathic scoliosis is a complex three-dimensional (3-D) deformity of the trunk, characterized by lateral deviation and axial rotation of the spine, usually accompanied by a rib cage deformity. Apart from their anomalous rotations, the individual vertebrae themselves become deformed. By analogy, the rib cage deformity does not only consist of changes in rib position and rib-vertebra angle but also of intrinsic rib deformations. The extent of these structural deformities is strongly related to the severity of the scoliotic curve.

It has long been recognized that mechanical forces can influence the shape of growing bone [16, 50, 55]. Animal studies have been performed in which changes of bone growth and bone remodelling were measured after alterations were made to the normal mechanical environment [5, 14, 19, 55]. In idiopathic scoliosis, whatever its primary cause, the normal physiological, biomechanical circumstances have been changed. Consequently, it would seem that the intrinsic vertebral and rib deformities develop secondary to scoliosis. Nevertheless, in the literature the intrinsic deformities have also been considered as primary aetiological factors [2, 34, 48].

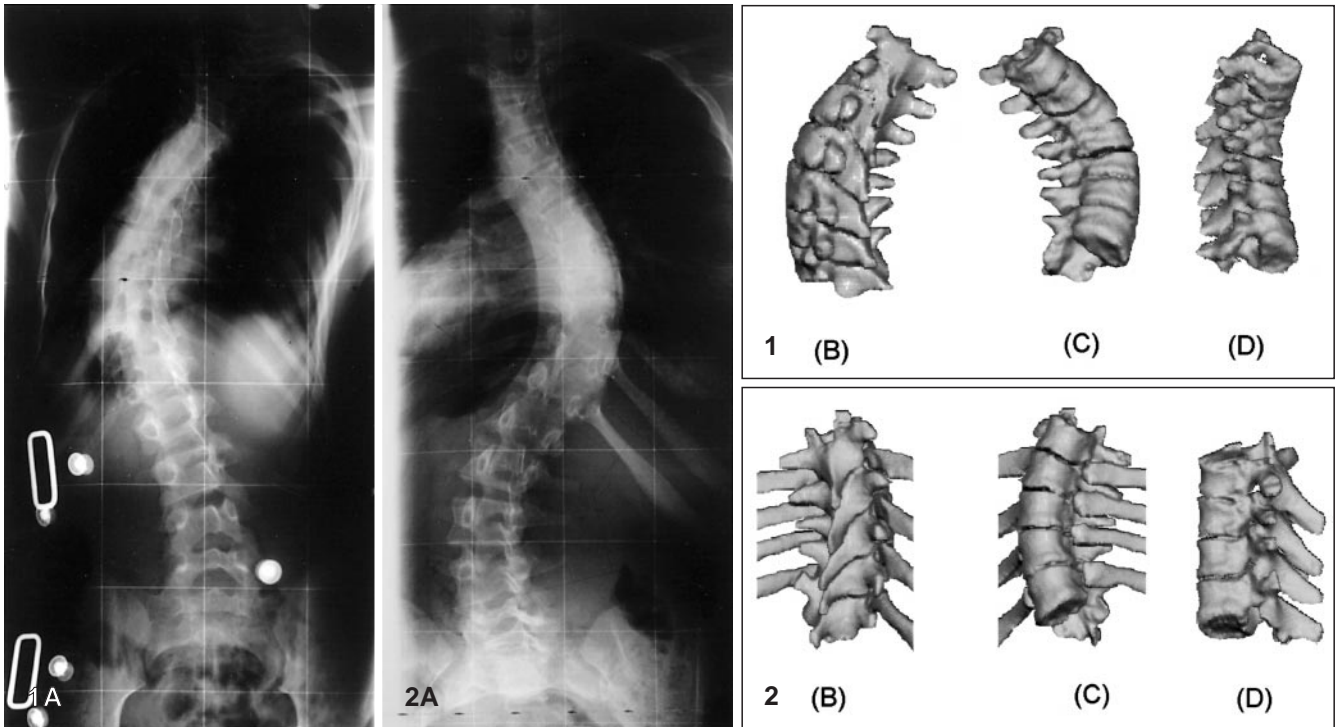


Fig. 1 Standing anteroposterior spinal radiograph (A) and posterior (B), anterior (C) and lateral (D) views of the 3-D CT reconstructions of the thoracic scoliotic segment of the first patient

Fig. 2 Standing anteroposterior spinal radiograph (A) and posterior (B), anterior (C) and lateral (D) views of the 3-D CT reconstructions of the thoracic scoliotic segment of the second patient

Many animal studies were performed to study the vertebral and rib deformities in experimentally induced scoliosis [18, 22, 28, 42–45]. However, it should be emphasized that in most of these studies the test animals were quadrupeds. An exception to these studies are those of chickens, where scoliosis, with characteristic vertebral deformities, was initiated through pinealectomy [7, 24, 51].

So far, the study of structural intrinsic vertebral deformities in patients with scoliosis has been limited to the wedge angle of the vertebral body on radiographs and the study of apical vertebrae of skeletons with a scoliotic deformity [3, 8, 10–13, 37, 39, 43]. Significant wedging has been measured on radiographs in scoliotic curves with a Cobb angle as small as 4° [56]. Many authors see this wedge deformation as an important explanation for the progression of scoliosis during the adolescent growth period [25, 37, 47]. Apart from this wedge deformation of the vertebral bodies, vertebral deformations are present in the transversal plane, including deformations of the spinous process, laminae and pedicles. Descriptions and biomechanical explanations of these deformations in the literature are limited and inconsistent [12, 42, 53].

The so-called rib hump is the most obvious component of the rib cage deformity in scoliosis. Measurements of

the rib-hump, rib-vertebra angle and descriptions of the complete deformed thorax in scoliosis can be found in the literature [1, 6, 21, 26, 46, 49, 56], but so far no clear description has been given of the individual intrinsic rib deformity.

Descriptions of the morphology of the intrinsic vertebral and rib deformations are essential for a better understanding of the deforming forces in the scoliotic spine and trunk. This knowledge is necessary for the development of new techniques in surgical correction and brace management. In the present study we were able to use axial CT of two patients with serious scoliosis and two specimens with a scoliotic deformity. Three-dimensionally rendered CT images of these scoliotic spines were used to describe the intrinsic vertebral and rib deformities in relation to their position in the scoliotic spine. A force system which may be held responsible for the development of these deformities will be discussed.

Material and methods

In the study we used axial spine CT (Philips SR 7000 Tomoscan) of two patients with serious idiopathic scoliosis. These examinations were performed for an extensive preoperative evaluation of a scoliosis correction including thoracoplasty. Slices were made every 2 mm in the scoliotic region. The first patient had a scoliotic spine with a single left curve, with its apex at the tenth thoracic vertebra. The Cobb angle on the standing anteroposterior radiograph measured 60° (Fig. 1A). The second patient had an S-shaped scoliotic spine with the thoracic curve to the right, with the apex at the tenth thoracic vertebra and a lumbar curve with its apex at the third lumbar vertebra. The thoracic Cobb angle measured

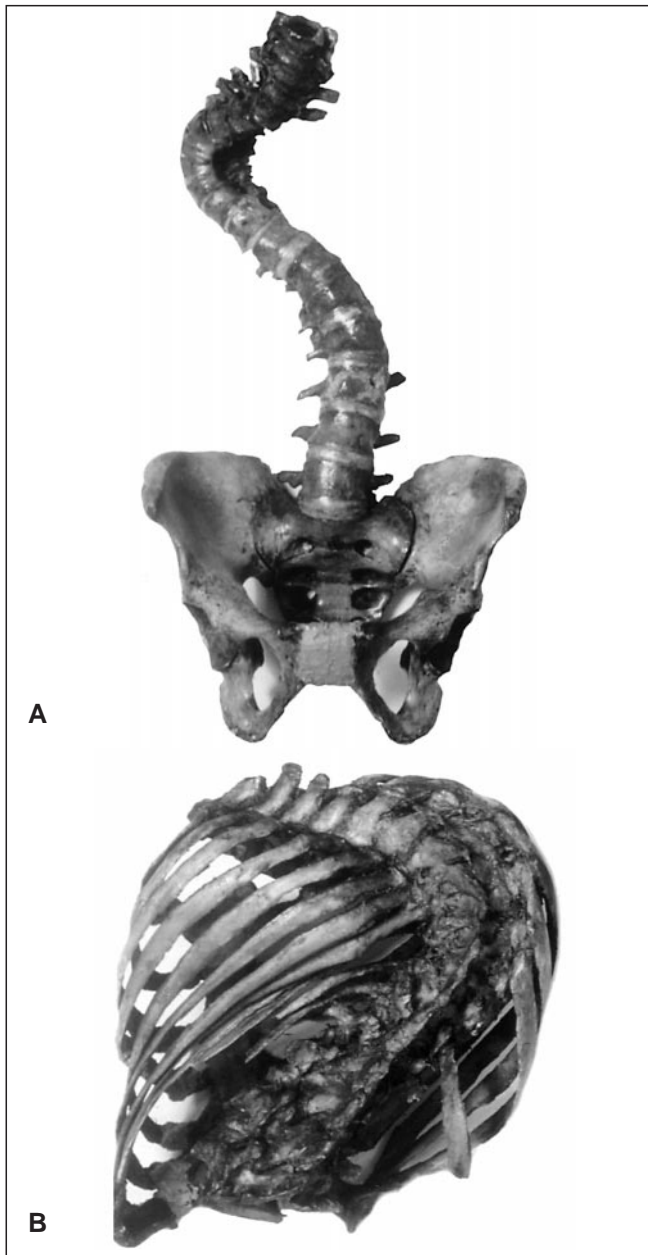


Fig. 3A, B Photographs of both skeletons. The photograph of the first skeleton shows an S-shaped scoliotic spine with the thoracic curve to the right (**A**). The photograph of the second skeleton shows a single right thoracic curve including deformed rib cage (**B**)

60° and the lumbar Cobb angle 50° (Fig. 2A). MRI of the spine of both patients revealed no indications of spinal tumours or any other pathology.

Two human skeletons with a scoliotic deformity were also studied by axial CT. Slices were made every 1 mm. The skeletons were borrowed from the Morbid Anatomy Museum of the Royal Free Hospital of London. The spine of the first skeleton was S-shaped, with the convexity of the thoracic curve to the right (Fig. 3A). The apices of the thoracic and lumbar curve were situated at the eighth thoracic vertebra and the third lumbar vertebra.

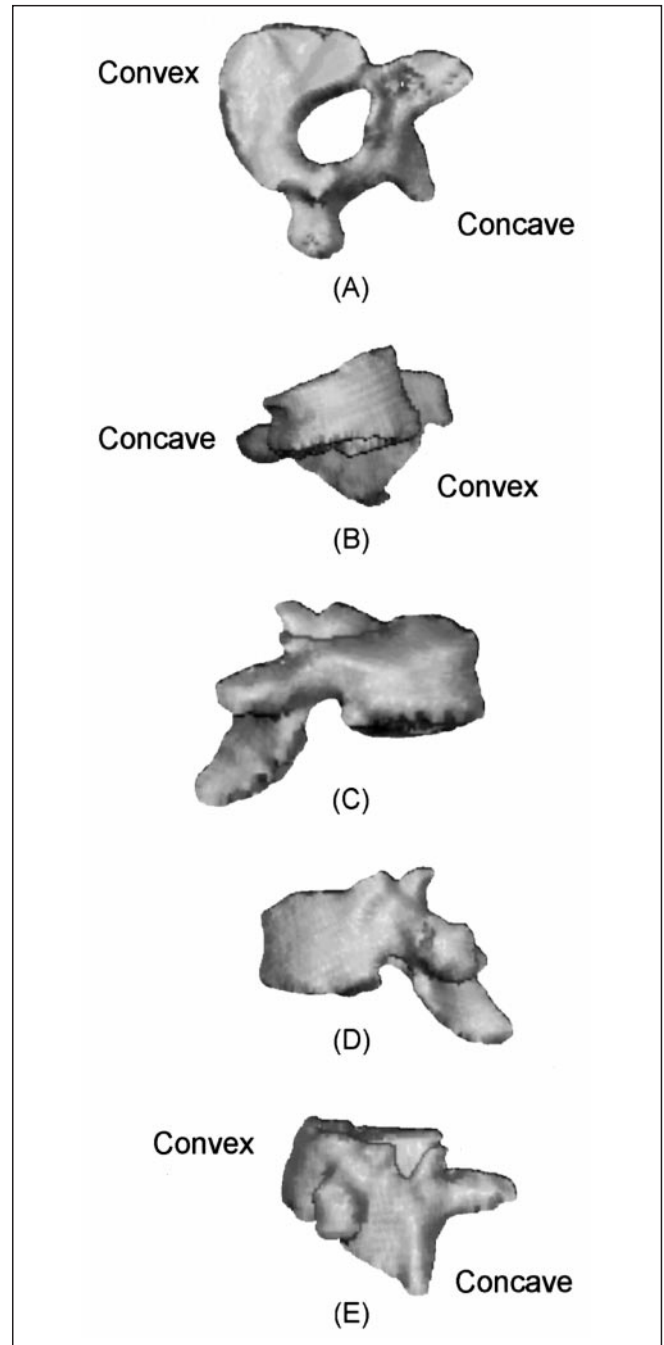


Fig. 4 Top view (**A**), anterior view (**B**), lateral-concave side (**C**) and lateral-convex side (**D**) views and posterior view (**E**) of the apical vertebra of the first patient. The anterior and lateral views have been corrected for the rotation of the vertebral body

The spine of the second skeleton (Fig. 3B) was a single right curve with the apex at the tenth thoracic vertebra. This spine was completely articulated with an intact rib cage. Neither skeleton showed any sign of tubercular foci, tumours or congenital anomalies. However, neuromuscular disturbance such as poliomyelitis, or other neuropathies or myopathies cannot be ruled out as the cause of scoliosis in these two skeletons.

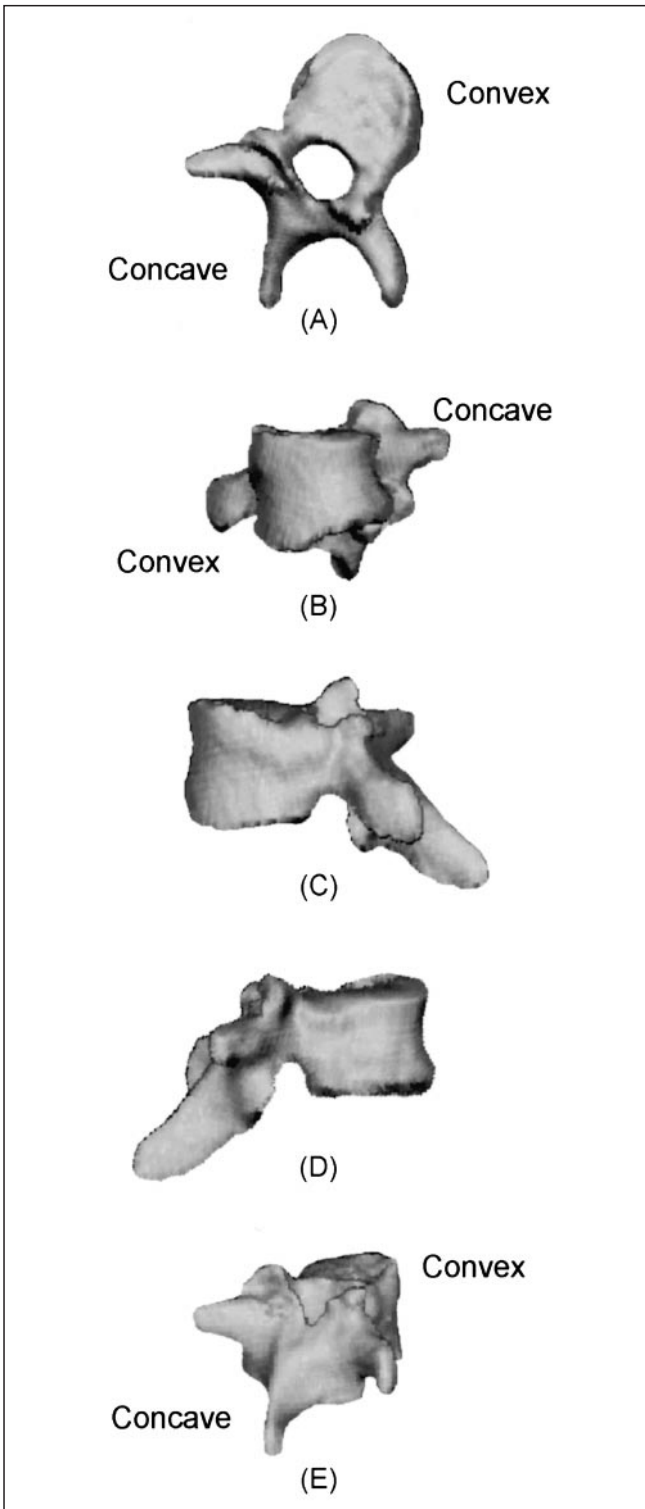


Fig. 5 Top view (A), anterior view (B), lateral-concave side (C) and lateral-convex side (D) views and posterior view (E) of the apical vertebra of the second patient. The anterior and lateral views have been corrected for the rotation of the vertebral body

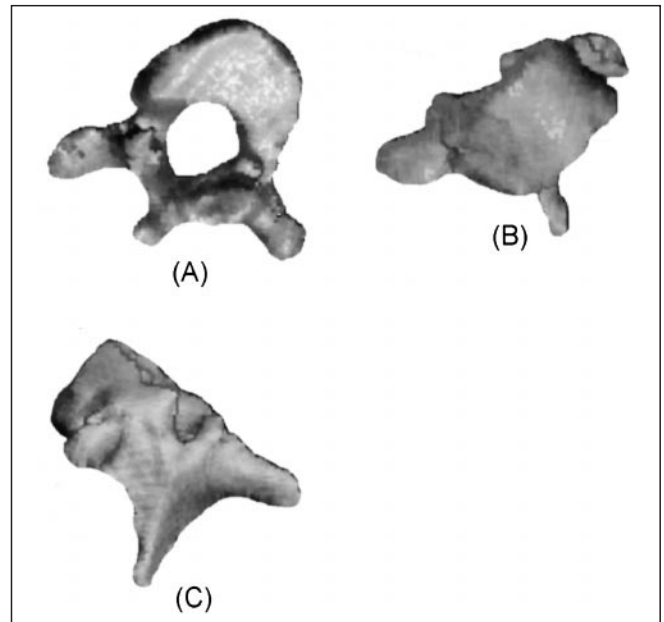


Fig. 6 Bottom view (A), anterior view (B), and posterior view (C) of the end vertebra of the first patient

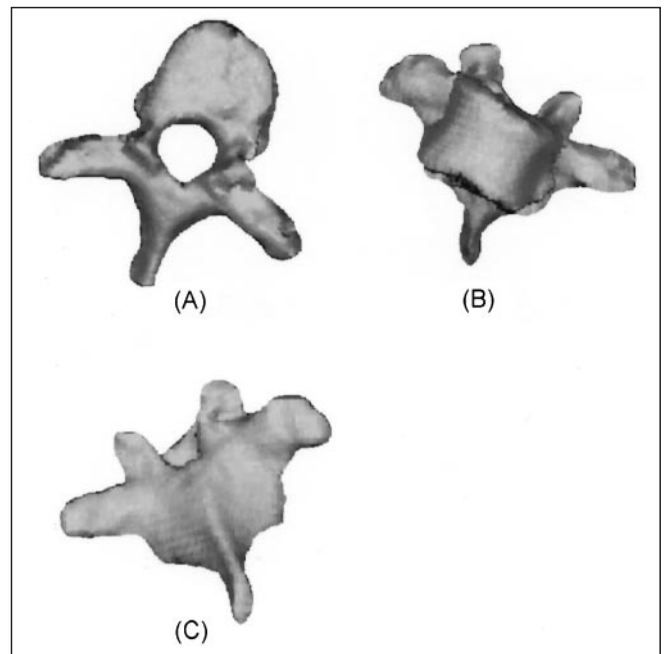


Fig. 7 Top view (A), anterior view (B), and posterior view (C) of the end vertebra of the second patient

Three-dimensional images were obtained by means of the axial CT examinations of the four scoliotic spines with Gyroview and Easy vision software (Philips). The 3-D reconstructions of the individual vertebrae and ribs were depicted from true coronal, sagittal and transversal views.

The analysis of the 3-D reconstructions concerned a morphological description of the intrinsic bony deformities of the vertebrae and ribs in relation to their position in the scoliotic spine.

Results

Vertebral deformities

The posterior, anterior and lateral views of the 3-D reconstructions of the thoracic scoliotic segment of the two patients in the study are shown in Fig. 1B–D and Fig. 2B–D. The anterior and posterior views demonstrate that the curve described by the vertebral bodies is significantly greater than the curve described by the spinous processes.

The top views of the apical vertebrae of both patients are shown in Figs. 4A and 5A. The deformity of the apical vertebra in the transversal plane consists of a gradual torsion between the posterior complex and the vertebral body. The vertebral body is maximally rotated towards the convexity of the scoliotic curve, whereas the tip of the spinous process is pointed to posterior. Moreover, an asymmetry of the pedicles can be observed. The pedicle at the convex side is thickened, whereas the concave pedicle is narrowed.

The anterior views of both apical vertebrae are shown in Figs. 4B and 5B. These are true anterior views of the apical vertebral body, since they have been corrected for the rotation of the vertebral body. This rotation was determined on the top views of the 3-D reconstructions. On the anterior views the wedge deformation of the apical vertebral bodies can be observed. This deformation is primarily characterized by an impression of the end plates on the concave side of the vertebral body.

The lateral views were also corrected for the rotation of the vertebral body. The true lateral views of the concave side of the apical vertebrae of both patients are shown in Fig. 4C and Fig. 5C. On these lateral views the impression on the concave side of the vertebral body may also be observed. The true lateral views of the convex side of the apical vertebrae demonstrate that both apical vertebral bodies have a tendency towards a slight bony lordotic deformation (Figs. 4D, 5D).

The posterior views of the apical vertebrae are shown in Figs. 4E and 5E. These images visualize the deformation of the posterior complex: the tip of the spinous process is pointed to posterior and then bends towards the convex side, causing the lamina and transverse process to show a rotation component.

The different views of the upper end vertebrae of the first and second patient are shown in Figs. 6 and 7 respectively. The bottom view of the first patient and the top view of the second patient show no torsion deformation, as was seen in the apical vertebrae. The anterior and posterior views of the upper end vertebrae show a slight torsion between the anterior and the posterior complexes. Here, in the coronal plane, the vertebral body is at a larger tilt than the posterior complex.

A study of the scoliotic specimens shows the same pattern in the vertebral deformities as with the patients. The bone formation at the concave side of the vertebral body is notable (Fig. 8).

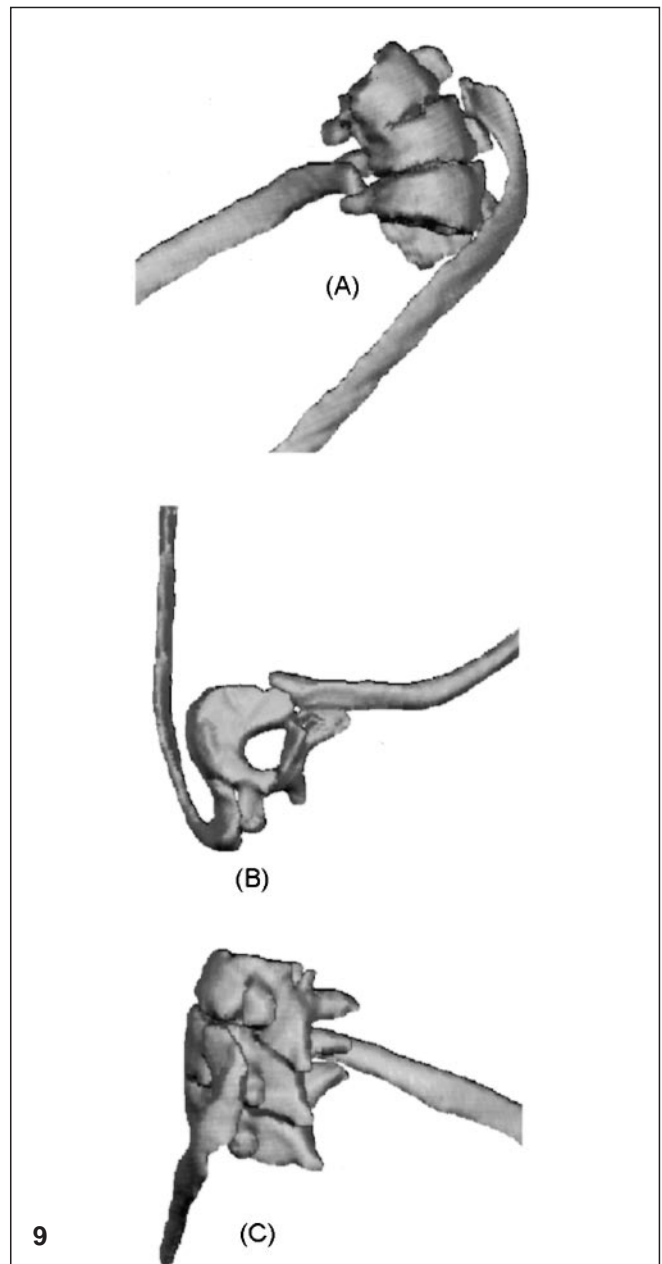
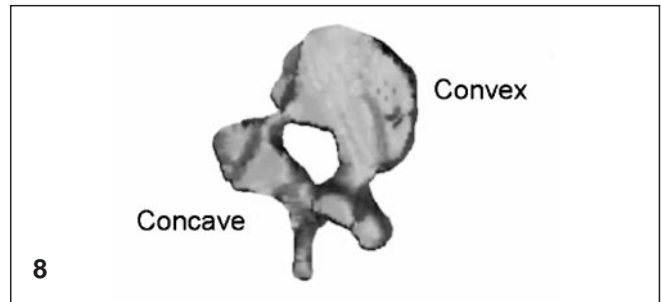


Fig. 8 Top view of the apical vertebra of the first skeleton

Fig. 9 The anterior (A), and top (B) posterior (C) views of the apical vertebrae and ribs of the first patient

sion forces in the posterior column. Resulting transversal components of the compressive column in the sagittal plane due to kyphosis or lordosis will primarily be resisted by the powerful musculo-ligamentous structures of the posterior spinal column [33].

In a scoliotic curve the direction of the compressive forces in the anterior spinal column has changed. In the frontal plane, the compressive forces at the apical level are inclined at an angle, which results in a shear force towards lateral (Fig. 10A). To achieve equilibrium in the scoliotic spine the lateral force components in the anterior column have to be counteracted by the musculo-ligamentous structures of the posterior column as well as bone elements such as the facet joints and ribs (Fig. 10B). However, should these structures fail to stabilize the scoliotic spine, for example during periods of growth, curve progression will occur.

The biomechanical differentiation between the anterior pressure column and the posterior tension column with scoliotic deformity was first made by Meijer in 1866 [27]. Other authors also stress the importance of "posterior tethering" with regard to the geometrical and morphological configuration of the scoliotic deformity [15, 23]. Various physical models and cadaver models are described, in which the posterior column functioned as a tension column with a strong tendency to shorten [4, 9, 17, 38]. For example, it was postulated that in scoliosis the growth rate of the anterior column is not in equilibrium with the lengthening of the musculo-ligamentous structures of the posterior column. This relative lengthening of the anterior components compared to the posterior elements is thought to result in a rotation in which the anterior column deviates more than the posterior column [10, 30, 40, 44]. However, it should be emphasized that these models do not explain the clinical observation that some cases of scoliosis show a marked progression, including serious intrinsic vertebra and rib deformities, whereas other cases stabilize at an early stage. It is possible that with serious progressive scoliosis the supportive musculo-ligamentous structures fail to stabilize the spine, or that the neuro-muscular control of these structures is deficient [42].

With the described force system, elastic deformations, but eventually also structural, plastic deformations, will occur. The bony plastic deformations, such as the intrinsic vertebral and rib deformities in scoliosis can be described by means of basic bone remodelling laws, such as Wolff's law and the law of Hueter-Volkman [16, 50, 55]. In the present study the deformity of the apical vertebra in the transversal plane consisted of a gradual torsion between the tip of the spinous process, the posterior complex and the vertebral body. The description of the deformity corresponds with those of Smith and Dickson [42]. The torsion deformities suggest that a significant lateral shear force operates on the vertebral body of the apical vertebrae. However, the posterior complex of the vertebrae attempts to retain its original position. This suggests that the

lateral shear force in the anterior column is counteracted by a torque, which is provided primarily by the musculo-ligamentous structures of the posterior part of the spinal column. Due to this torque, compressive and tension forces will occur on the convex and concave pedicles respectively (Fig. 10B). According to Wolff's law this causes the convex pedicle to shorten and to thicken, as shown in the present study.

At the end vertebrae, i.e. the vertebrae with the largest horizontal tilt, a small torsion was found between the anterior and the posterior complexes in the coronal plane. Here the vertebral body was at a larger tilt than the posterior complex. This deformation in the coronal plane suggests that it is caused by the properties of the posterior column, since the powerful ligamentous and muscular structures of the posterior column attempt to minimize the horizontal tilt of the end vertebrae.

Like Stilwell and Smith et al. we found in both scoliotic specimens some bone growth on the concave side of the vertebral body [43, 45]. This appositional bone growth, also described in literature as bone-drift, is probably the result of increased longitudinal pressure at the concave side of the vertebral body. This increased pressure is also responsible for the wedge deformation of the apical vertebral bodies in the coronal plane. The bone growth at the concave side of the vertebral body in the transversal plane and the wedge deformation are an expression of the paradox between Wolff's law and the law of Hueter-Volkman: an increased pressure in the growth direction results in a decreased longitudinal epiphyseal growth (wedge deformation), but also in an increase in appositional bone growth.

Deacon and Dickson reported that the height of the anterior vertebral body of the apical vertebrae was significantly greater than the posterior vertebral body height [8, 9, 11, 29]. This lordosis at bone level was an important basis for their theory that thoracic lordosis, which is caused by a relative overgrowth of the anterior part of the vertebral body, triggers the initiation of scoliosis. A minimal wedge deformation in the local sagittal plane was also observed in certain apex vertebrae in the present study. Still the question remains whether this deformation in the sagittal plane is a primary aetiological phenomenon, as Deacon and Dickson suggest, or a secondary phenomenon, caused by the deforming forces in the scoliotic spine, comparable to the vertebral deformations described above.

The thoracic spine is closely connected to the rib cage through the costo-vertebral joints. These consist of the costo-transverse joints and joints between the head of the rib and the vertebral body. The greatest curve of the normal rib is situated at the posterior angle. Proximal of the posterior angle the rib inclines superomedially while beyond the angle the rib continues in an even curve, sloping down until it reaches the costal cartilage [54]. The observed intrinsic rib deformities on the convex side of the scoliotic curve showed an increased angulation of the rib curve at the pos-

terior angle and a torsion of the most proximal part of the rib. This torsion around the longitudinal axis reveals itself in an increased rib-vertebra angle, as is shown on the anteroposterior radiograph. The rib deformity on the concave side consisted of a flattening of the rib curve.

The resulting lateral forces of the anterior column on the thorax are greatest at the most proximal end of the convex ribs and may cause an increase in the rib curvature at the posterior angle. The torsion deformity possibly arises through the relative torsion slackness of the rib structure. Consequently, the visualized rib deformities suggest that they develop secondary to scoliosis, due to lateral forces induced by the scoliotic spine.

Conclusion

In scoliosis a force system arises which may be held responsible for the geometrical and morphological charac-

teristics of scoliosis. In this study the focus was on the intrinsic bony vertebral and rib deformities in scoliosis. The visualized deformities suggest that these are caused by bone remodelling processes due to forces in the anterior spinal column, which drive the apical vertebral body out of the midline, and forces of the musculo-ligamentous structures of the posterior column, which attempt to minimize the deviations and rotations of the vertebrae. The demonstrated rib deformities suggest an adaptation to the lateral forces imposed by the scoliotic spine.

Acknowledgements This work was supported by STW (Netherlands Technology Foundation). We gratefully acknowledge P. Mook from the Department of Radiology, University Hospital of Groningen, and A. Huitema and B. Verdonck from Philips Medical Systems, Best, for their assistance in obtaining the 3D CT reconstructions.

References

1. Aaro S, Dahlborn M (1981) The longitudinal axis rotation of the apical vertebra, the vertebral, spinal, and ribcage deformity in idiopathic scoliosis studied by computer tomography. *Spine* 6: 567–572
2. Agadir M, Sevastik B, Sevastik J, Persson A, Isberg B (1988) Induction of scoliosis in growing rabbits by unilateral growth stimulation of the ribs. *Spine* 13:1065–1069
3. Arkin AM (1949) The mechanism of the structural changes in scoliosis. *J Bone Joint Surg Am* 31:519–528
4. Arkin AM (1950) The mechanism of rotation in combination with lateral deviation in the normal spine. *J Bone Joint Surg Am* 32:180–188
5. Arkin AM, Katz JF (1956) The effects of pressure on epiphyseal growth. The mechanism of plasticity of growing bone. *J Bone Joint Surg Br* 38:1056–1076
6. Closkey RF, Schultz AB (1993) Rib cage deformities in scoliosis: spine morphology, rib cage stiffness, and tomography imaging. *J Orthop Res* 11: 730–737
7. Coillard C, Rivard CH (1996) Vertebral deformities in scoliosis. *Eur Spine* 5:91–100
8. Deacon P, Flood BM, Dickson RA (1984) Idiopathic scoliosis in three dimensions. A radiographic and morphometric analysis. *J Bone Joint Surg Br* 66:509–512
9. Deacon P, Archer IA, Dickson RA (1987) The anatomy of spinal deformity: a biomechanical analysis. *Orthopedics* 10:897–903
10. Deane G, Duthie RB (1973) A new projectional look at articulated scoliotic spines. *Acta Orthop Scand* 44:351–365
11. Dickson RA, Lawton JO, Archer IA, Butt WP (1984) The pathogenesis of idiopathic scoliosis. Biplanar spinal asymmetry. *J Bone Joint Surg Br* 66:8–15
12. Enneking WF, Harrington P (1969) Pathological changes in scoliosis. *J Bone Joint Surg Am* 51:165–184
13. Farkas A (1954) The pathogenesis of idiopathic scoliosis. *J Bone Joint Surg Am* 36:617–654
14. Haas SL (1945) Retardation of bone growth by a wire loop. *J Bone Joint Surg* 27:25–33
15. Herzenberg JE, Waanders NA, Closkey RF, Schultz AB, Hensinger RN (1989) Cobb angle versus spinous process angle in adolescent idiopathic scoliosis. The relationship of the anterior and posterior deformities. *Spine* 15:874–879
16. Hueter C (1862) Anatomische Studien an den Extremitätengelenken Neugeborener und Erwachsener. *Virchows Arch* 25: 572–599
17. Jarvis JG, Ashman RB, Johnston CE, Herring JA (1987) The posterior tether in scoliosis. *Clin Orthop* 227:126–134
18. Karaharju EO (1967) Deformation of vertebrae in experimental scoliosis. The course of bone adaptation and modelling in scoliosis with reference to the normal growth of the vertebra. *Acta Orthop Scand Suppl* 105:1–87
19. Karaharju EO, Ryöppy SA, Mäkinen RJ (1976) Remodelling by asymmetrical epiphysial growth. An experimental study in dogs. *J Bone Joint Surg Br* 58: 122–126
20. Klein JA, Hukins DWL (1983) Functional differentiation in the spinal column. *Eng Med* 12:3–18
21. Kristmundsdottir F, Burwell RG, James JLP (1985) The rib-vertebra angles on the convexity and concavity of the spinal curve in infantile idiopathic scoliosis. *Clin Orthop* 201:205–209
22. Langenskiöld A, Michelsson JE (1961) Experimental progressive scoliosis in the rabbit. *J Bone Joint Surg Br* 43: 116–120
23. Lindahl O, Raeder E (1962) Mechanical analysis of forces involved in idiopathic scoliosis. *Acta Orthop Scand* 32: 27–38
24. Machida M, Dubouset J, Imamura Y, Miyashita Y, Yamada T, Kimura J (1996) Melatonin: a possible role in pathogenesis of adolescent idiopathic scoliosis. *Spine* 21:1147–1152
25. Mente PL, Stokes IAF, Spence H, Aronsson DD (1997) Progression of vertebral wedging in an asymmetrically loaded rat tail model. *Spine* 22: 1292–1296
26. Metha MH (1972) The rib-vertebra angle in the early diagnosis between resolving and progressive infantile scoliosis. *J Bone Joint Surg Br* 54:230–243
27. Meyer GH (1866) Die Mechanik der Skoliose. *Arch Pathol Anat Physiol Klin Med* 35:15–253

28. Michelsson JE (1965) The development of spinal deformity in experimental scoliosis. *Acta Orthop Scand Suppl* 81:1–91
29. Millner PA, Dickson RA (1996) Idiopathic scoliosis: biomechanics and biology. *Eur Spine J* 5:362–373
30. Murray DW, Bulstrode CJ (1996) The development of idiopathic scoliosis. *Eur Spine J* 5:251–257
31. Nachemson AL (1981) Disc pressure measurements. *Spine* 6:93–97
32. Nachemson AL (1966) The load on lumbar discs in different positions of the body. *Clin Orthop* 45:107
33. Nijenbanning G (1998) Scoliosis redress. Thesis, University of Twente
34. Normelli H, Sevastik JA, Akrivos J (1985) The length and ash weight of the ribs of normal and scoliotic persons. *Spine* 10:590–592
35. Oda I, Abumi K, Lü D, Shono Y, Kaneda K (1996) Biomechanical role of the posterior elements, costovertebral joints, and rib cage in the stability of the thoracic spine. *Spine* 21:1423–1429
36. Panjabi MM (1992) The stabilizing system of the spine. I. Function, dysfunction, adaptation and enhancement. *J Spinal Disord* 5:383–389
37. Perdriolle R, Becchetti S, Vidal J, Lopez P (1993) Mechanical process and growth cartilages. Essential factors in the progression in scoliosis. *Spine* 18:343–349
38. Roaf R (1958) Rotation movements of the spine with special reference to scoliosis. *J Bone Joint Surg Br* 40:312–332
39. Roaf R (1960) Vertebral growth and its mechanical control. *J Bone Joint Surg Br* 42:40–59
40. Roaf R (1966) The basic anatomy of scoliosis. *J Bone Joint Surg Br* 48:786–792
41. Rolander SD (1966) Motion of the lumbar spine with special reference to the stabilizing effect of the posterior fusion. Thesis, Department of Orthopaedic Surgery, University of Gothenburg
42. Smith RM, Dickson RA (1987) Experimental structural scoliosis. *J Bone Joint Surg Br* 69:576–581
43. Smith RM, Pool RD, Butt WP, Dickson RA (1991) The transverse plane deformity of structural scoliosis. *Spine* 16:1126–1129
44. Somerville EW (1952) Rotational lordosis: the development of the single curve. *J Bone Joint Surg Br* 34:421–427
45. Stilwell DL (1962) Structural deformities of vertebrae. Bone adaptation and modelling in experimental scoliosis and kyphosis. *J Bone Joint Surg Am* 44:611–634
46. Stokes IAF, Dansereau J, Moreland MS (1989) Rib cage asymmetry in idiopathic scoliosis. *J Orthop Res* 7:599–606
47. Stokes IAF, Spence H, Aronsson DD, Kilmer N (1996) Mechanical modulation of vertebral body growth. Implications for scoliosis progression. *Spine* 21:1162–1167
48. Taylor JR (1983) Scoliosis and growth: patterns of asymmetry in normal vertebral growth. *Acta Orthop Scand* 54:596–602
49. Thulbourne T, Gillespie R (1976) The rib hump in idiopathic scoliosis. Measurement, analysis and response to treatment. *J Bone Joint Surg Br* 58:64–71
50. Volkmann R (1882) Verletzungen und Krankheiten der Bewegungsorgane. In: von Pitha FR, Billroth Th (eds) *Handbuch der allgemeinen und speziellen Chirurgie*, Bd 2, Teil 2. Ferdinand Enke, Stuttgart
51. Wang X, Jiang H, Raso J, et al (1997) Characterization of the scoliosis that develops after pinealectomy in the chicken and comparison with adolescent idiopathic scoliosis in humans. *Spine* 22:2626–2635
52. White AA, Panjabi MM, Thomas CL (1977) The clinical biomechanics of kyphotic deformities. *Clin Orthop* 128:8–17
53. White AA, Panjabi MM (1990) Clinical biomechanics of the spine, 2nd edn. J.B. Lippincott, Philadelphia, pp 128–168
54. Williams PL, Bannister LH, Berry MM, et al (1995) *Gray's anatomy*, 38th edn. Churchill Livingstone, Edinburgh
55. Wolff J (1986) The law of bone remodelling. Springer, London
56. Xiong B, Sevastik JA, Hedlund R, Sevastik B (1994) Radiographic changes at the coronal plane in early scoliosis. *Spine* 19:159–164